Influence of roughness on initial in vitro response of cells to Al2O3/Ce-TZP nanocomposite

Marta Suárez (m.suarez@cinn.es)
Centro de Investigacion en Nanomateriales y Nanotecnologia
Silvia Pérez-López
Sespa
Catuxa Prado
Healtsens
Adolfo Fernández
Centro de Investigacion en Nanomateriales y Nanotecnologia
José Serafín Moya
Centro de Investigacion en Nanomateriales y Nanotecnologia
Ramón Torrecillas
Centro de Investigacion en Nanomateriales y Nanotecnologia
Luis Antonio Díaz
Centro de Investigacion en Nanomateriales y Nanotecnologia

Research Article

Keywords: Nanocomposites, roughness, biocompatibility, Al2O3/Ce-TZP

Posted Date: July 22nd, 2020

DOI: https://doi.org/10.21203/rs.3.rs-44864/v1

Abstract

Al_2O_3/Ce-TZP nanocomposite has been synthetized by a colloidal processing route and sintered in air atmosphere. The roughness surface of ATZ nanocomposite by sandblasting using materials with different particle size has been modified and its influence on the osteogenic differentiation has been performed in vitro growing a human osteoblast-like cell line, SaOs-2, and Human Adipose-derived mesenchymal stem cells (hADMSC). The non-cytotoxicity and haemocompatibility of ATZ nanocomposite has been proved. An increase in the expression of BGLAP and IBSP genes was observed on samples sandblasted with white corundum (< 90 μm) whereas SPARC gene was upregulated on samples sandblasted with SiC (90–100 μm). Alumina-ceria-stabilized zirconia nanocomposite presented in this work exhibits a high potential for application in the fabrication of dental implants due to their biological behaviour and very promising mechanical properties.

1. Introduction

During more than 40 years, commercially pure titanium and titanium alloys were widely used as dental implant materials due to their excellent biocompatibility, early osseointegration and high corrosion resistance [1]. Nevertheless, titanium may induce allergic reactions or sensitivities [2] and it possesses a dark color that could be exposed during peri-implant mucosa recession and ruin the entire aesthetic result [3]. As a viable alternative to resolve these problems, some new ceramic materials were developed. Bioceramic materials offer excellent opportunities to combine the absence of metal ions, good bone ingrowth characteristics and improved aesthetics due to the possibility of dying the product with pigments. In this context, alumina (Al_2O_3) was the first bioceramic used as an implant material [4], due to its low friction, wettability, wear resistance and biocompatibility. However, it showed insufficient physical properties. In the 80 s, zirconia (ZrO_2) emerged as a ceramic material valid for implants because of its improved fracture toughness and mechanical strength with respect to alumina. Tetragonal zirconia polycrystals, specially 3 mol% yttria-stabilized zirconia (3Y-TZP), serves as a metal substitute in substrates and possesses good physical characteristics; its bending strength doubles and its fracture toughness almost triples that of alumina [5]. Nevertheless, the big disadvantage of pure 3Y-TZP is its low temperature degradation (LTD) [6]. Actually, combining the positive properties of Al_2O_3 (wear resistance, hydrothermal stability and hardness) with those of ZrO_2 (strength and fracture toughness) it is possible to obtain Alumina Toughened Zirconia (ATZ) and Zirconia Toughened Alumina (ZTA) nanocomposites with a higher potential for application as dental implants [7]. Among them, composite materials with Ce-TZP and alumina have shown very promising mechanical properties to be used in the fabrication of implants [8]. Besides the mechanical properties of the bulk material, the characteristics of an implant's surface, such as composition, topography and roughness play an important role in cell-material integration and biocompatibility [9]. The interaction between cells and a biomaterial's surface is fundamentally relevant and essential in terms of the response of cells at the interface, affecting the growth and quality of newly formed bone tissue [10, 11]. For this reason cell culture models are routinely used to study the response of osteoblastic cells in contact with different substrates for implantation in

bone tissue. Moreover, Human Adipose-derived mesenchymal stem cells (hADMSC) are considered to contain a group of pluripotent mesenchymal stem cells and manifest multilineage differentiation capacity, including osteogenesis, chondrogenesis and adipogenesis [12]. These last cells could differentiate into odontogenic lineage, expressing bone marker proteins, and might be used as suitable seeding cells for tooth regeneration [13]. Few data are available concerning the response of mesenchymal stem cells to ATZ. The purpose of the present study was to perform in vitro osteogenic differentiation assays growing a human osteoblast-like cell line, SaOs-2, and hADMSCs on different ATZ supports in order to determine the influence of the composition and roughness surface on the behavior of the cells in relation with these new implants. In this context, different tests were performed to study cytotoxicity, viability, haemolysis and differences in terms of osteogenic and apoptotic gene expression between the samples.

2. Materials And Method

The Al_2O_3/Ce-TZP nanocomposite was made using the following materials: Ce-TZP (10mol% CeO_2) from Daichi (Japan) with an average particle size of 35 nm (d_{50}) and a specific surface area of 15 $m^2.gr^{-1}$, α-Al_2O_3 powder (TM DAR, Taimei Chemical Co., Japan) with a specific surface area of 14.6 $m^2.gr^{-1}$ and an average particle size (d_{50}) of 150 nm. In addition, the following chemical precursors were also used: i) aluminum chloride (Sigma-Aldrich, Spain), ii) zirconium IV-propoxide (70% solution in 1-propanol) (Sigma-Aldrich, Spain), iii) 2-Propanol (99.9% Panreac, Spain) and iv) absolute ethanol (99.97% Panreac, Spain). The colloidal processing route to obtain this nanocomposite is described in Rivera et al [14] and L. A. Díaz et al [15].

2.1. Disk specimen preparation

The powders were cold isostatically pressed at 300 MPa into cylindrical rods of 50 mm in length and 9 mm in diameter. After surface machining and firing at 1475ºC for one hour, disk-shaped specimens of 7 mm diameter and 1.3 mm thickness were prepared by cutting and polishing (applying microcrystalline diamonds of 9, 3 and 1 microns). In total, 36 disks for sandblasting tests and six more as target specimens were used.

2.2. Sandblasting process

Disks were sandblasted with white corundum and SiC powders (see Table 1). Laser diffraction (Beckman Coulter LS 13 320, USA) was used for the granulometric characterization of the selected fractions. The air pressure was applied perpendicular to the surface of the disk at 0.4 bars and at a distance of 10 mm using sandblaster equipment (Sandblaster I, Astursinter, Spain).

Samples	Sandblasting material
Sample NA	Non sandblasted sample (control)
Sample A	Sandblasted by: White Corundum < 90 µm, 60 s
Sample B	Sandblasted by: 90 µm < SiC < 250 µm, 15 s
Sample C	Sandblasted by: SiC < 90 µm, 15 s

Table 1: Sample references and materials used for surface treatment.

2.3. Surface roughness and morphology

The morphology of the samples and the raw materials used in the process of sandblasting was characterized by Field Emission Scanning Electron Microscopy (FESEM) (FEI: Quanta FEG 650, USA). The surface roughness of the specimens was analyzed using a surface roughness tester (MicroTest: MT4002, Spain). Six measurements on each specimen according to ISO 4287-1997 [16] were performed. The assessed profile (Ra) as an arithmetical mean deviation was calculated. The amount of transformation (monoclinic volume content) induced by sandblasting was determined by X-ray diffraction (XRD) (Bruker D8 Advance, Germany) using the method of Toraya et al. [17]. This behavior was studied with a Tuttnauer Autoclave (2540EL, Tuttnauer, NY, USA) following ISO 13356:2015 [18].

2.4. In vitro studies methodology

Different tests were carried out in order to assess the biocompatibility, non-cytotoxicity and haemocompatibility of the Al_2O_3/Ce-TZP nanocomposite:

- Human Adipose-derived mesenchymal stem cells (hADMSCs) isolation and culture: hADMSCs were isolated from abdominal subcutaneous adipose tissue. Adipose tissue was submitted to mechanical digestion and then digested with Collagenase I (Sigma-Aldrich, USA) DMEM solution (Lonza, Belgium) and the cell suspension was filtered and centrifugated. The obtained cell fraction was cultured in expansion medium to 80% confluence, at 5% CO_2 and 37ºC. Finally, cells were harvested using Trypsin-EDTA 1X (Biowest, France).
- Citotoxicity tests using the Neutral Red Uptake (NRU) assay and the MTS assay. The potential cytotoxic effect of materials on mammalian cells was determined following ISO 10993-part 5 [19] for biomaterials and medical device testing. Samples were sterilized before use. SaOs-2 cells (human osteosarcoma cells, kindly provided by the SCT of the University of Oviedo, Spain) or human MSCs from adipose tissue were seeded onto 48-well plates at a density of approximately $4{\cdot}10^4$ cells/ml/cm^2 and cultured until achieving confluence. Then, samples were placed in contact with the cell

monolayer. In the NRU test, the uptake of NR into the lysosomes/endosomes and vacuoles of living cells is used as a quantitative indication of viability. Cells were washed after 24h and incubated with neutral red solution (Scharlab, Spain) for 3h. After that, cells were washed again and NR was desorbed by adding a mixture of ethanol and acetic acid. The amount of NR extracted from the cells was measured at 540nm and the percentage of viable cells was calculated as Eq. (1).

$$\%\ \text{of viable cells} = 100 \times {\text{Abs}_{540}(\text{extract})}\Big/{\text{Abs}_{540}(\text{blank})} \quad (1)$$

In the MTS assay, culture medium was removed after 24h and fresh medium with MTS solution (CellTiter 96® AQueous One Solution Cell Proliferation Assay, Promega, USA) (5:1) was added to each well. After 3-4 additional hours in the presence of MTS, absorbance was determined at 490nm and the percentage viability was calculated as Eq. (2).

$$\%\ \text{of viable cells} = 100 \times {\text{Abs}_{490}(\text{extract})}\Big/{\text{Abs}_{490}(\text{blank})} \quad (2)$$

- Haemolysis index (norm ASTM F 756-08 [20]): Hb released into plasma when blood was exposed to the materials was measured: After a period of incubation, samples were removed and tubes were centrifuged. Each supernatant (100µL) were mixed with Drabkin`s reagent (100µL) and cyanmethemoglobin was produced and detected by spectrophotometry at 540 nm. Total blood hemoglobin (TBH) was also measured. The hemolytic index was calculated as Eq. (3).

$$\text{Hemolytic Index} = {\text{Hb released}\ \left(\frac{\text{mg}}{\text{mL}}\right)}\Big/{\text{TBH}\ \left(\frac{\text{mg}}{\text{mL}}\right)} \quad (3)$$

- Osteogenic differentiation of SaOs-2 (human osteoblast-like cell line) and hADMSCs: Cells were seeded at a density of 50 x 10^3 cells on each of the four kinds of samples until confluence and cultured in differentiation medium supplemented with dexamethasone, ascorbic acid and β-glycerol phosphate (all reagents from Sigma-Aldrich, USA). Every 72h, differentiation medium was changed, and in 3 weeks, the whole differentiation process was completed. In order to confirm the adequate osteogenic differentiation, Alkaline phosphatase and Alizarin red staining were performed.

- Alkaline phosphatase staining: Differentiated osteogenic cells were fixed with formaldehyde (Merck, Germany), stained with a BCIP/NBT solution (SIGMA FAST™ BCIP/NBT, Sigma-Aldrich, USA) and observed by microscopy.
- Alizarin red staining: Differentiated osteogenic cells were fixed with paraformaldehyde, stained with alizarin red solution (Merck, Germany) and observed by microscopy.
- RNA extraction and cDNA synthesis: Total RNA was isolated using Tri reagent® solution (Ambion, USA). After evaluating the quality of the RNA through absorbance measurements, each RNA sample was reverse transcribed to obtain cDNA samples.
- Real-Time quantitative polymerase chain reaction: Quantitative PCR was performed using a CFX96 Real-Time System (Bio-Rad, Hercules, CA, USA). Fluorescence data during the primer extension step were acquired. The melting-curve analysis, to confirm product specificity, was performed immediately after amplification, following 1 min of denaturation at 95°C, 1 min of annealing at 65°C and 60 cycles of 0.5°C increments (30 sec each) beginning at 65°C while monitoring fluorescence. β-ACTIN was used as the endogenous control. ALPL, BGLAP, COL1, IBSP and SPARC are bone differentiation genes and CASPASE 3 are used as an indicator of apoptotic damage. B-ACTIN was used as a normalized gene.
- Statistical analysis: Data using the Proc MIXED procedure of the SAS/STAT v8.2 software package (SAS Institute, Inc., Cary, NC, USA) were statistically analyzed. *C*t values (number of cycles needed to generate a fluorescent signal above a predefined threshold) and Δ*C*t values (difference between the *C*t of the target gene and that of the housekeeping gene) for each gene and repetition were used as dependent variables. To quantify gene expression levels a relative standard method was used. The model fitted included the type of sample as the fixed effect and the sample as a random effect to account for the non-independency of the repetitions. For each sample level, least-square means and their corresponding standard errors were computed. For descriptive purposes, a Student's *t* test t on raw *C*t means computed for samples using Proc GLM of SAS/STAT was also carried out, assuming that the sample type effect included two independent groups of normally distributed observations.

3. Results

3.1. FESEM

Fig. 1 shows the representative microstructure of the sintered ATZ nanocomposite. Two different phases can be observed. The lightest one corresponds to the Ce-TZP matrix with a particle size of 400-500nm and the darkest phase corresponds to alumina with an average size of 250nm. As it can be observed alumina grains are homogeneously distributed and no pores are observed.

3.2. Surface roughness

Sandblasting is a commonly used surface treatment and involves impacting with hard particles at high velocities on a surface in order to erode it and leave a roughened surface with expected higher wettability. FESEM micrographs of the modified ATZ surfaces by sandblasting with white corundum and silicon carbide for 90s and 15s are shown in Figure 2A-C. Sandblasting with white corundum and SiC particles <90 microns (Fig. 2 A and C, respectively), revealed a regular and slightly waved structure. However, the surface of the sandblasted ATZ with SiC particles between 90 and 250μm (Fig.2B) showed more irregular structure with visibly larger voids and grooves, increasing the surface roughness according to the results shown in Table 2 for ATZ samples. The mean roughness index, Ra, in case of samples sandblasted with SiC between 90 and 250 microns was significantly higher than the other sandblasted samples. According to the Altbrektsson and Wennerberg classification [21], the samples sandblasted with white corundum present a “smooth” surface roughness (Ra < 0,5 μm), while the samples sandblasted with SiC show “minimally rough” and “moderately rough” surface roughness. Similar results has been found by Sato et al. [22] where sandblasting by SiC particles resulted in surface roughness values larger than those by alumina particles.

Raw materials	Ra < 0.5 μm	0.5 μm < Ra < 1.0 μm	1.0 μm < Ra < 2.0μm	Ra > 2.0 μm
	Smooth*	Minimally rough*	Moderately rough*	Rough*
W.C.< 90 μm	0.465 ± 0.06			
SiC 250-90μm			1.358 ± 0.11	
SiC < 90 μm		0.580 ± 0.08		
N. S	0.031 ± 0.10			

Table 2: Roughness values of the ATZ nanocomposite surfaces after sandblasting with corundum and SiC for 90 and 15 seconds (mean ± SD in μm).N.S (No Sandblasting).

3.3. XRD diffraction

The volumetric fraction of the monoclinic phase was measured on: (1) as-sintered surfaces, (2) as-sintered surfaces after sandblasting process, (3) as-sintered surfaces after sandblasting and its ageing process. As it can be seen in Table 3, the materials do not present spontaneous phase transformation on their surface after sintering and any ageing process. However, sandblasting

processes leads to the transformation, under tension, of a part of the tetragonal zirconia to monoclinic zirconia. According to the results shown in Table 3, the particle size and the kind of material used for the sandblasted process have an effect on the transformation phase of ATZ composite [23]. Increasing the particle size increases the erosion of material and the transformation surface layer. This transformation process is reversible and, in every case, a posterior thermal treatment at 1200ºC for 15 minutes succeeds in transforming the totality of the monoclinic zirconia back to its initial tetragonal state [24].

Treatment	Monoclinic phase content ($V_{m\ total}$)
ATZ as-sintered	3,80% ±3%
ATZ as-sintered and ageing during 5h	2,10% ±3%
ATZ as-sintered sandblasting surface by white corundum < 90 µm, 60 s	24,73% ±3%
ATZ as-sintered sandblasting surface by white corundum < 90 µm 60 s ageing during 5h	27,00% ±3%
ATZ as-sintered sandblasting surface by SiC 250-90 µm, 15 s.	48,70% ±3%
ATZ as-sintered sandblasting surface by SiC 250-90 µm, 15 s ageing during 5h	50,00% ±3%
ATZ as-sintered sandblasting surface by SiC <90 µm, 15s	31,70% ±3%
ATZ as-sintered sandblasting surface by SiC <90 µm, 15 s ageing during 5h	36,00% ±3%

Table 3: Volumetric fractions of monoclinic phase zirconia present on different sandblasted surfaces.

3.4. In vitro biological assays

ISO 10993-5 [19] states that a material is considered non-cytotoxic when cell viability is above 70%. The potential cytotoxicity on SaOs-2 and hADMSCs was assessed by the MTS assay and the NRU method using tissue culture polystyrene (TCPS) as the blank. According to the results shown in Fig. 3A-B all of the studied samples allowed for higher than 90% cell viability, therefore, none of the surface modification treatments can be considered cytotoxic.

Haemolysis is the alteration, dissolution or destruction of red blood cells that results in hemoglobin liberation into the surrounding medium. According to Stanley´s classification criteria, a material is considered non-hemolytic for hemolytic indexes <2 while it is considered slightly hemolytic and hemolytic for hemolytic index values of 2-5 and >5, respectively. Different factors such as surface roughness, surface energy and surface tension and surface wettability can have an influence on the blood compatibility and it is shown that surface modification has a great potential for improving the hemocompatibility of biomedical materials and devices [25]. In this case, the studied ATZ nanocomposite showed a hemolytic index close to 0 (0.1-0.2) for all the surface modifications tested, which was <1% indicating nonhemolytic material.

ALP levels increase when active bone formation (osseous differentiation) occurs, as it is a by-product of this process. According to the results shown in Fig. 4 A and B a correct osteoblast differentiation of hADMSCs has been taken placed since all of the differentiated cells used for gene expression studies were stained and, consequently, osteoblast differentiation confirmed.

Product identity was confirmed by electrophoresis on ethidium bromide-stained 2% agarose gels in 1X TBE buffer, which resulted in a single product of the desired length. In addition, an iCycler iQ melting curve analysis was performed, which rendered single product specific melting temperatures. No primer-dimers were generated during the 40 real-time PCR cycles conducted. All polymerase chain reaction efficiencies were above 90% and linearity was high, with correlation coefficients (R^2) above 0.989.

To quantify gene expression, the relative standard method (relative fold changes) was used and expression levels were determined for the ceramics and the control group (NA sample) by normalizing results with respect to β-ACTIN. For hADMSCs, a discreet increase was noticed in the relative expression of four of the studied genes for samples A, B and C when compared with the control sample. In Fig. 5, these increases are plotted. In the problem group, the genes BGLAP, CASPASE 3, IBSP and SPARC were up-regulated 2.27-fold for sample A, 1.57-fold for sample C, 3.10-fold for sample A, and 2.27-fold for sample B, respectively, with respect to the basal levels recorded for the endogenous control (β-ACTIN). However, these increases were only significant ($p<0.05$) in the case of IBSP for sample A.

In the case of the SaOs cells, an even more discreet increase was observed in the relative expression of two of the studied genes for samples A, B and C when compared with the NA sample (control). These results are also shown in Fig. 5. The IBSP gene is 1.55-fold up-regulated for sample B. The COL1A1 gene is up-regulated 2.95-fold for sample A, 2.85-fold for sample B and 1.74-fold for sample C with respect to the basal levels recorded for the endogenous control. In this case, differences between control and problem groups were not significant.

4. Discussion

The Alumina Toughened Zirconia (ATZ) biomaterial studied in this work is a nanocomposite that combines the properties of Al_2O_3, such as wear resistance, hydrothermal stability and hardness, with the strength and fracture toughness of Ce-ZrO_2. Moreover, Ce-TZP does not suffer low temperature degradation. The good combination of mechanical properties of this nanocomposite has already been proven [14] and now it is necessary to confirm its good interaction with cells. The ideal material to make implants should not be purely tolerated by the host but should interact with biological systems in a way that induces the appropriate host response for a specific application [26]. The host response towards a biomaterial is dictated by the cells that respond to the biomaterial which, in turn, is controlled by the proteins that coat the surface of the biomaterial. Importantly, the nature and activity of the proteins adsorbed on the surface depend on the physical and chemical properties of the surface. Therefore, cell

behavior depends indirectly on surface characteristics, which should be appropriate to actively promote an adequate and specific host response. For instance, for the efficacy of dental implants it is essential to establish intimate contact between the biomaterial's surface and bone structure elements; therefore, the biomaterial should permit cell adhesion, promote proliferation and avoid detrimental responses such as induction of cell death or inflammation. Cell attachment and adhesion phenomena belong to the first stages of material-cell interactions and will influence the capacity of cells to spread, proliferate and differentiate. Importantly, adherent cells (like osteoblasts and fibroblasts) do not divide and even undergo apoptosis in case of adhesion deprivation [27]. Therefore, these early events strongly contribute to generate a successful host response and must be studied in research endeavors directed to develop new biomaterials for the design of bone contact implant devices. Biomaterial surface specifications can influence adsorption of biological molecules and, in the second stage, cell response. In fact, the biomaterial’s surface properties, such as topography and hydrophilicity will be determinant in terms of biocompatibility and other biological phenomena. Over the years, in order to improve their wear properties, corrosion resistance and biocompatibility to biomaterials surface modifications have been applied. A series of studies has indicated that roughness stimulates the adhesion, growth and osteogenic differentiation of mesenchymal stem cells (MSCs). In the literature, surfaces with $Ra \leq 1$ μm are considered smooth and those with $Ra > 1$ μm are described as rough. In general, the surface roughness range that favours osseous differentiation has been reported to be 1.0-1.5 μm [28]. In the present study, SaOs-2 cells and hADMSC cells were used to investigate the influence of roughness on regulation of cell viability, hemolysis and osseous differentiation. According to the results obtained in the cytotoxicity and heamolysis experiments, the data obtained in our study revealed that there are no significant differences in the responses of osteogenic cells and hADMSCs towards the different surface modification treatments in terms of biocompatibility. In fact, none of the surface modification treatments induced significant cell death in osteoblasts, hADMSC or erytrocytes. Similar results regarding cell viability and hemolysis have been published over the years [29]. Given the bioinertness of ceramic materials, such as those studied in this work, treatments to modify the surface and provide a suitable environment are necessary in order to trigger a favorable biological response in terms of osseous differentiation. Concerning gene expression, different osteogenic genes were studied in order to determine differences between samples. For hADMSCs the increase was only lightly observed in the case of four genes BGLAP, CASPASE3, IBSP and SPARC. BGLAP was up-regulated 2.27-fold for sample A, CASPASE3 was up-regulated 1.57-fold for sample C, IBSP was up-regulated 3.10-fold for sample A and, finally, SPARC was up-regulated 2.27-fold for sample B with respect to the basal levels. However, the increase was only significant ($p < 0.05$) in the case of IBSP in sample A. These findings in terms of gene expression as well as histological results showed that the roughness and the nature of the material are adequate to allow cells to achieve osteogenic differentiation, despite the fact that the surface roughness of the studied samples is clearly below the Ra values reported to favor osseous differentiation (1.0-1.5 μm). It is important to note that osteoblastic differentiation of MSCs into functional differentiated osteoblasts requires a series of steps involving the expression of different proteins at each stage. Alkaline phosphatase is regarded as a marker of early osteoblastic differentiation. In fact, it is the main signal that compromises cells to differentiate towards osteoblastic lineage; in a similar way, COL1 gene is over-expressed in the pre-osteoblastic phase

coinciding with the beginning of the bone tissue-differentiating cascade, whereas secretion of Osteocalcin and IBSP as well as matrix mineralization is associated with the final differentiation phase. The observation of an increasing expression of IBSP with significant differences between groups for white corundum (sample A) showed that the differences in terms of osteogenic differentiation seem not to appear until the last phases, meaning that the gene expression pattern is similar for all samples during the entire process. Significantly, the main increase observed in IBSP is in agreement with the results obtained by Wang and cols [30] that pointed out the importance of the integrin-linked kinase/β-catenin pathway in mediating signals from topographic cues to direct the osteogenic differentiation of cells. For SaOs-2 cells, the three samples (A, B and C) showed upregulation related to sample NA (control) for two of the studied genes, IBSP and COL1. However, this upregulation was not signification any case. The expected pattern for SaOs-2 cells is clearly different from that of hADMSC because it is a human osteoblast-like cell line itself and it is supposed to express osteogenic genes such as COL1 at the beginning of the bone tissue differentiating cascade or IBSP that are over expressed at middle-to-late osteogenic differentiation. These observations are in agreement with Czekanska et al. [31], who described high levels of expression of osteocalcin, bone sialoprotein, decorin and procollagen-I. For both types of cells (hADMSCs and SaoS), the apoptotic gene studied, Caspase-3, did not show important differences between samples, meaning that neither material nor roughness had a clear influence on cell death. This circumstance is in agreement with the absence of deleterious effects on cell viability.

4. Conclusions

The non-cytotoxicity and haemocompatibility of a nanocomposite ceramic material formed by alumina and ceria stabilized zirconia has been proved. The surface roughness of this nanocomposite can be adjusted depending on the particle size of the materials used for sandblasting. Smooth roughness values of around 0.5 μm are obtained when the abrasive material (white corundum or silicon carbide) is below 90 μm, while the use of silicon carbide particles of sizes between 90 and 250 μm leads to surface roughness values of around 1.5 μm. Moreover, the roughness and the nature of the material used have been proved adequate for cell osteogenic differentiation. An increase in the expression of BGLAP and IBSP genes was observed on samples sandblasted with white corundum below 90 μm, whereas SPARC gene was upregulated on samples sandblasted with SiC between 90 and 250 μm. Then, the studied nanocomposite is a very promising material for dental applications thanks to its good mechanical properties in comparison with conventional ceramics, the possibility of adjusting its surface roughness and the different in vitro results obtained.

Declarations

Acknowledgments

The Spanish Ministry of Science, Innovation and Universities and the Spanish Higher Council for Scientific Research (CSIC) have supported this research under the Projects MAT2012-38645 and INPERIO,

H2020-SMEInst-2018-2020-2 Ref CSIC-20185222 respectively. Catuxa Prado acknowledges financial support from the JAE-DOC program (CSIC).

Electronic Supplementary Material

Supplementary material correspond to Tables S1-S12 is available in the online version of this article.

References

1. Sidambe TA (2014) Biocompatibility of Advanced Manufactured Titanium. Implants—A Review Materials 7:8168–8188
2. Sicilia A, Cuesta S, Coma G et al (2008) Titanium allergy in dental implant patients: a clinical study on 1500 consecutive patients. Clin Oral Implants Res 19:823–835
3. den Hartog L, Raghoebar GM, Slater JJH et al (2013) Single-Tooth Implants with Different Neck Designs: A Randomized Clinical Trial Evaluating the Aesthetic Outcome. Clin Implant Dent Relat Res 15:311–321
4. Schulte W (1976) The Tubinger immediate implant. Quintessenz 27:17–23
5. Garvie RC, Hannink RH, Pascoe RT (1975) Ceramic steel? Nature 258:703–704
6. Chevalier J, Gremillard L, Deville S (2007) Low-Temperature Degradation of Zirconia and Implications for Biomedical Implants. Annu Rev Mater Res 37:1–32
7. Chevalier J, Gremillard L (2009) Ceramics for Medical Applications: A Picture for the Next 20 Years. J Eur Ceram Soc 29:1245–1255
8. Benzaid R, Chevalier J, Saâdaoui M et al (2008) Fracture toughness, strength and slow crack growth in a ceria stabilized zirconia–alumina nanocomposite for medical applications. Biomaterials 29:3636–3641
9. Wennerberg A, Albrektsson T, Andersson B (1995) An animal study of c.p. titanium screws with different surface topographies. J Mater Sci Mater Med 6:302–309
10. Lamers E, Frank Walboomers X, Domanski M et al (2010) The influence of nanoscale grooved substrates on osteoblast behavior and extracellular matrix deposition. Biomaterials 31:3307–3316
11. Pae A, Lee H, Kim H-S,. Kwon Y-D, Woo Y-H (2009) Attachment and growth behaviour of human gingival fibroblasts on titanium and zirconia ceramic surfaces. Biomed Mater 4:025005
12. Liu TM, Martina M, Hutmacher DW, Hui JHP, Lee EH, Lim B (2001) Identification of Common Pathways Mediating Differentiation of Bone Marrow- and Adipose Tissue-Derived Human Mesenchymal Stem Cells into Three Mesenchymal Lineages. Stem Cells 25:750–760
13. Jing W, Wu L, Lin Y, Liu L, Tang W, Tian W (2008) Odontogenic differentiation of adipose-derived stem cells for tooth regeneration: necessity, possibility, and strategy. Med Hypotheses 70:540–542

14. Rivera S, Diaz L, Fernández A, Torrecillas R, Moya J. Reinforcement Mechanisms in Alumina Toughened Zirconia Nanocomposites with Different Stabilizing Agents. 2014;34:15–22
15. Díaz LA, Torrecillas R. Material compuesto nanoestructurado de circona estabilizada con ceria y alúmina dopada con circona, procedimiento de obtenión y usos. ES. Patent 2 351 759 A1, Feb. 2011
16. ISO 4287:1997 (1997) Geometric Product Specification (GPS). In: Surface Texture Profile Method: Terms, Definition and Surface Texture Parameters. Int. Org. Stand, Geneva
17. Toraya H, Yoshimura M, Somiya S (1984) Calibration Curve for Quantitative Analysis of the Monoclinic-Tetragonal ZrO2 System by X-Ray Diffraction. J Am Ceram Soc 67:C–C119
18. ISO 13356: 2015, Implants for surgery- Ceramic Materials Based on Yttria-Stabilized Tetragonal Zirconia (Y-TZP). International Organization for Standarization, 2008
19. ISO 10993-5:2009 Biological evaluation of medical devices–part 5: Tests for in vitro cytotoxicity. International Organization for Standardization, 2009
20. ASTM F756–08. Standard Practice for Assessment of Hemolytic Properties of Materials. American Society of Testing Materials, 2008
21. Albrektsson T, Wennerberg A (2004) Oral implant surfaces: Part 1 - Review focusing on topographic and chemical properties of different surfaces and in vivo responses to them. Int J Prosthodont 17:536–543
22. Sato H, Yamada K, Pezzotti G, Nawa M, Ban S (2008) Mechanical Properties of Dental Zirconia Ceramics Changed with Sandblasting and Heat Treatment. Dent Mater J 27:408–414
23. Sato H, Ban S, Nawa M, Suehiro Y, Nakanishi H (2007) Effect of Grinding, Sandblasting and Heat Treatment on the Phase Transformation of Zirconia Surface. Key Eng Mater 330–332:1263–1266
24. Tanaka K, Tamura J, Kawanabe K et al (2003) Phase stability after aging and its influence on pin-on-disk wear properties of Ce-TZP/Al2O3 nanocomposite and conventional Y-TZP. J Biomed Mater Res A 67:200–207
25. Huang N, Yang P, Leng YX et al (2003) Hemocompatibility of titanium oxide films. Biomaterials 24:2177–2187
26. Williams DF. Definitions in biomaterials: proceedings of a consensus conference of the European Society for Biomaterials; 1986 March 3–5; Chester, England. Elservier;1987
27. Straface E, Natalini B, Monti D et al (1999) C3-Fullero-tris-methanodicarboxylic acid protects epithelial cells from radiation-induced anoikia by influencing cell adhesion ability. FEBS Lett 454:335–340
28. Hempel U, Hefti T, Kalbacova M, Wolf-Brandstetter C, Dieter P, Schlottig F (2010) Response of osteoblast-like SAOS-2 cells to zirconia ceramics with different surface topographies. Clin Oral Implants Res 21:174–181
29. Gautam C, Joyner J, Gautam A, Rao J, Vajtai R (2016) Zirconia based dental ceramics: structure, mechanical properties, biocompatibility and applications. Dalton T 45:19194–19215

30. Wang W, Zhao L, Wu K et al (2013) The role of integrin-linked kinase/β-catenin pathway in the enhanced MG63 differentiation by micro/nano-textured topography. Biomaterials 34:631–640
31. Czekanska EM, Stoddart MJ, Richards RG, Hayes JS (2012) In search of an osteoblast cell model for in vitro research. Eur Cells Mater 24:1–17

Figures

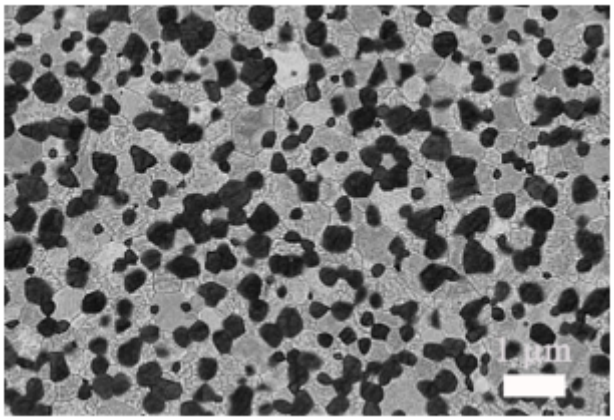

Figure 1

FESEM microstructure of polished surface of the ATZ nanocomposite

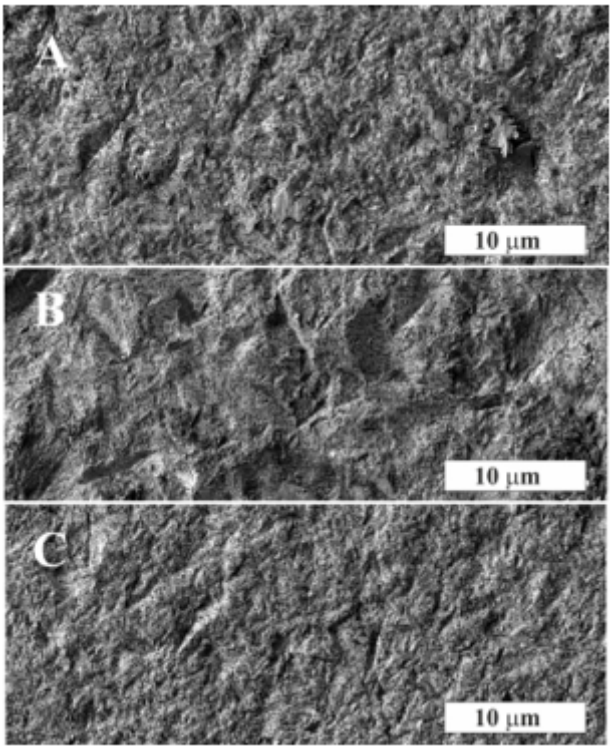

Figure 2

FESEM images from the topographical appearance of sandblasted surfaces with white corundum and silicon carbide raw materials. A) White corundum < 90 mm time: 60 s; B) SiC < 250 mm and > 90 mm time: 15 s; and C) SiC < 90 mm time 15 s.

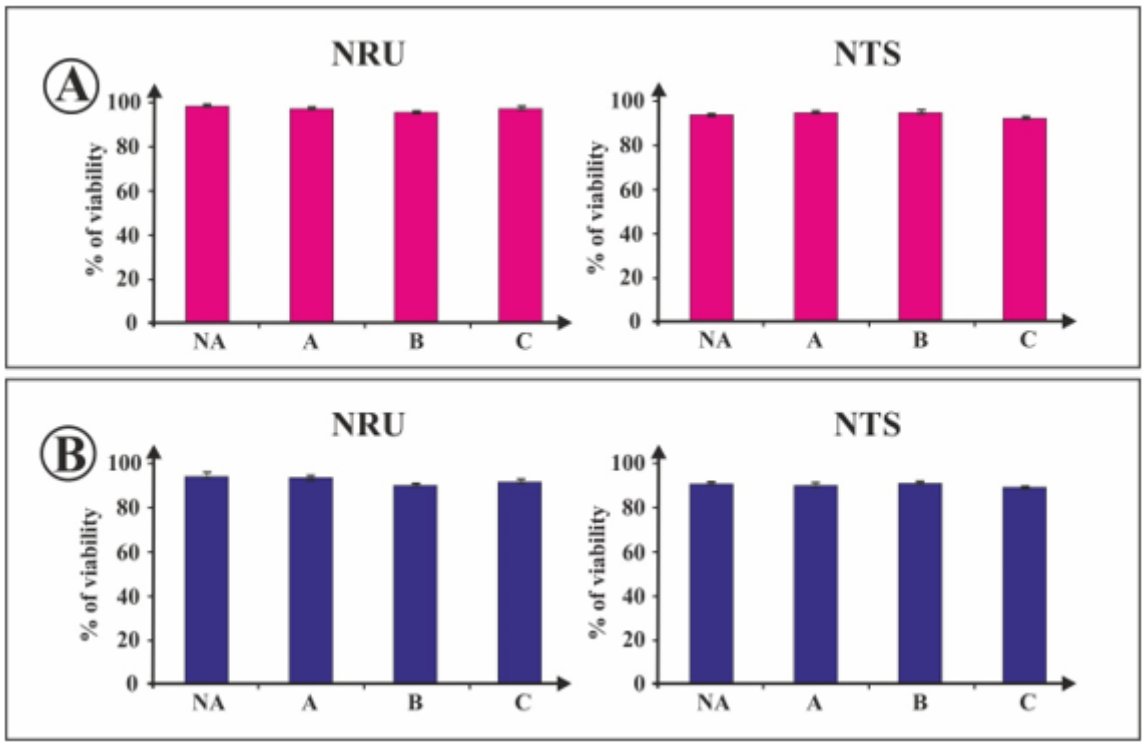

Figure 3

Biological assessment: NRU and MTS assay. No reduction in cell viability was observed for either the SaOs-2 (A) or the hADMSC (B) cells for any of the surface modifications tested, since the percentage viability was always superior to 70 %. Bars represent the means (SD) of triplicate measurements.

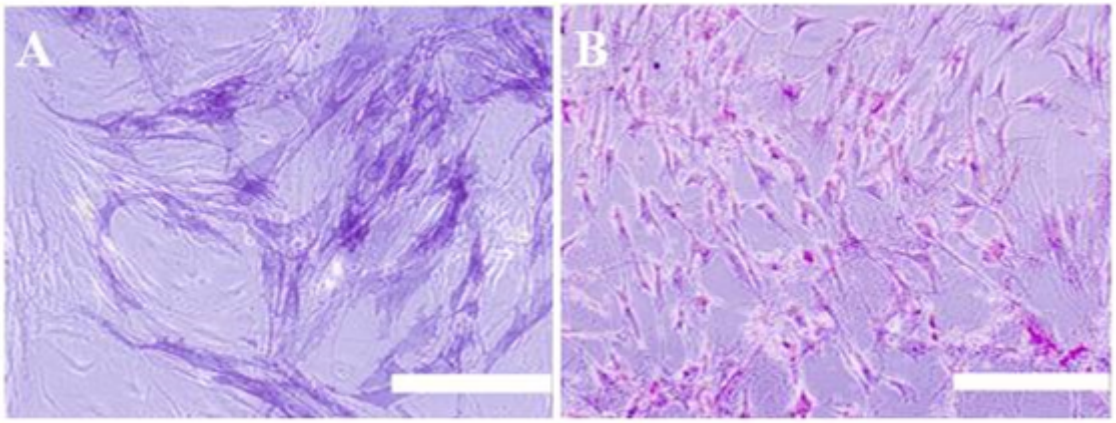

Figure 4

Alkaline phosphatase staining (A) and Alizarin red staining (B). White bar represent 500 µm

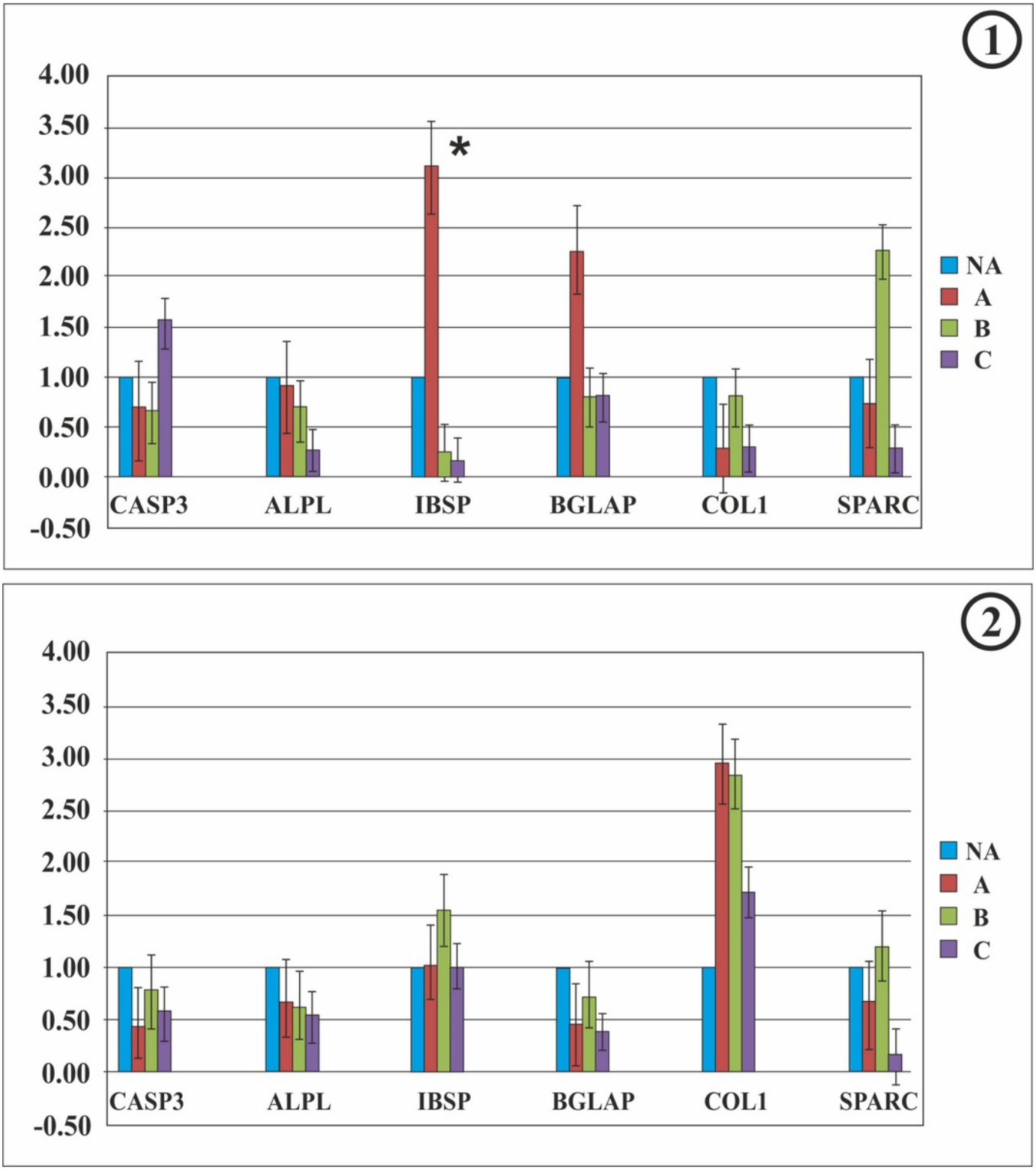

Figure 5

Relative quantification of the studied genes. mRNA levels for apoptotic and bone differentiation genes recorded in hADMSCs (upper part) and SaOs-2 cells relative to endogenous control gene β-ACTIN levels. Values are expressed as mean ± SEM. * indicates a significant difference with respect to the controls at p less than 0.05.

Supplementary Files

This is a list of supplementary files associated with this preprint. Click to download.

- SupplementaryMaterial.odt